possible impact crater (25 km in diameter) is situated slightly below the middle of Fig. 2 (6.5° longitude, 56.9° latitude).

Toward the south, the Maxwell Montes region and Lakshmi Planum merge into Sedna Planitia. The steepness of the slope in the southern portion of Lakshmi Planum (Vesta Rupes) is greater than 10°. In the northern portion the folds come together in a winding "plait," which descends to an altitude of 2 km over a distance of more than 500 km in the meridional direction and then merges into the plain. This is a southern part of the vast plain close to the pole that was discovered by Venera 15 and Venera 16. In the northern and southern parts of this region (Fig. 2) are numerous cone-shaped features standing out especially clearly on the background of smooth surface relief. These cones are most likely of volcanic origin.

REFERENCES AND NOTES

1. The image contains 1350 vertical lines, each having 195 points. The slant range and radial velocity relative to the spacecraft were calculated for each point of the image; for this purpose the data for distance and velocity with respect to the Venus center of mass were used. The lines and points are separated from each other by 800 m, which is slightly less than the radar spatial resolution (~1 km). For obtaining the same contrast of surface features in the regions of high and low reflectivity, the power of the reflected signal was normalized to the mean value in the window (160 km) running along the swath.
2. The processing of the radar altimeter reflected signals yielded the spacecraft altitude over the mean surface of the strip (40 km long, 7 km wide) with a root-mean-square error of about 50 m, the step along the ground track being 3 km. This error characterizes the relative accuracy of the relief height determination at over a distance of 500 to 1000 km along the track. At the ends of a track, as well as between tracks, the error may be 10 times larger. Considerable deviations of the local radius from the value of 6051 km, which is considered the radius of the sphere on which the image is plotted, resulted in appreciable perspective distortions in the crater configuration that were also taken into account while plotting the radar altimeter track on the image.
3. The radar image bands for each day of the survey were plotted on the sphere of 6051 km radius (venusian coordinate system) and then projected onto the cone surface drawn between two standard parallels. In accordance with the International Astronomical Union, the right ascension of the Venus rotation north pole is taken as 273.8°, the declination as 67.2°, and the period of rotation as 243.01 days. Zero meridian position of the venusian coordinate system is defined from the observation that, on 20 June 1964 at 0 hours ephemeric time, the longitude of Venus' central meridian was 320°. On a contour map the measured height values were reproduced directly on the altimeter track, whereas between the tracks they were interpolated.
4. Radar surveys by the spacecraft Pioneer Venus [H. Masursky *et al.*, *J. Geophys. Res.* **85**, 8332 (1980)] showed that Maxwell Montes is the most elevated region on Venus, although low spatial resolution made the analysis of their nature difficult. The general structure of the central part of the mountainous region together with Cleopatra Patera was visible on the radar images obtained recently from Earth at the Arecibo facility [D. B. Campbell, in *Abstracts of the Twenty-fifth Plenary Meeting of COSPAR* (Graz, Austria, 1984), p. 69]. However, the surrounding areas having smoother surfaces were less visible because of the low level of reflected signal. When Venus is observed from Earth (taking into account the large distance), the angle between the incident ray and the local vertical is equal to the venusian latitude, which is 60° to 70° for Maxwell Montes. From the Venera 15 and Venera 16 radar survey, the incident angle is from 9° to 15°. Therefore backscattering has a high intensity, and the surface features are observed fairly well throughout the map (Fig. 2). As a rule, the reflected signal does not drop below the level that exceeds the noise power of the receiving equipment by 10 decibels. This gives a uniform quality of radar images in regions with both high and low reflectivity.
5. The height of the local relief and corrections to the spacecraft coordinates were taken into consideration. The spacecraft coordinates were specified in accordance with the procedure that considers disturbances in the parameters at the time when the astro-orientation system is being switched on. Comparison with Fig. 1, where the image was constructed on the sphere of 6051 km radius, shows that taking into account the height of the local relief leads to cancellations of the image distortions that are particularly observable in the Cleopatra Patera region.
6. In the initial construction of the contour map, the measurements were averaged in a running window with a 100-km effective diameter, which caused smoothing of the relief [V. A. Kotelnikov *et al.*, *Pis'ma Astron. Zh.* (*U.S.S.R.*) **10**, 883 (1984)].
7. According to the Pioneer Venus altimeter data, the highest point of Maxwell Montes lies 220 km farther south (longitude 2.2°, latitude 63.8°), its height being 11.1 km (also above the level of the mean sphere of radius 6051 km)[H. Masursky *et al.*, *J. Geophys. Res.* **85**, 8332 (1980)].

8 July 1985; accepted 7 November 1985

X-ray Diffraction from Magnetically Oriented Solutions of Macromolecular Assemblies

Marc J. Glucksman, R. D. Hay, Lee Makowski

A simple system was developed for obtaining x-ray diffraction patterns from magnetically oriented solutions of macromolecular assemblies. A small permanent magnet was designed that produces a magnetic field of 16 kilogauss in a volume of 1 cubic millimeter and is mountable on most x-ray cameras. Many subcellular structures have sufficient diamagnetic anisotropy that they exhibit orientation in dilute solution when placed between the poles of the magnet. Diffraction from solutions oriented in this magnet can provide substantially more structural information than small-angle scattering from isotropic solutions. In favorable cases, such as dilute solutions of filamentous bacteriophages, it is possible to produce oriented fiber diffraction patterns from which intensities along layer lines can be measured to 7-angstrom resolution. The magnetically induced birefringence observed in solutions of other macromolecular assemblies suggests that this technique may have broad applicability to subcellular structures.

Most macromolecular assemblies exhibit sufficient diamagnetic anisotropy (*1*) that they become oriented in a magnetic field of moderate strength (10 to 20 kG). These include such widely diverse structures as the filamentous bacteriophages (*2–4*), whole retinal rods (*5*), fibrin (*6*), purple membrane (*7*), nucleic acids (*8*), and sickle cell hemoglobin fibers (*9*). Orientation of these assemblies in solution has usually been characterized by measurement of magnetically induced birefringence or neutron diffraction. Whereas small-angle diffraction from isotropic solutions produces a one-dimensional data set containing limited information, diffraction from an oriented solution produces a two-dimensional data set that can provide detailed information about molecular structure (*10*). Consequently, x-ray diffraction from magnetically oriented solutions has the potential to produce more structural information than conventional solution scattering.

Technical problems have made x-ray diffraction studies of solutions in a magnetic field difficult. For example, the magnet geometry is usually incompatible with the geometric requirements of x-ray cameras. High-quality x-ray diffraction patterns require the x-ray source, focusing optics, specimen, and film (or detector) to be within a few centimeters of each other. This is difficult to achieve when the specimen is between the poles of a large electromagnet or surrounded by the Dewar of a superconducting magnet. Furthermore, a weak fringe magnetic field will deflect the electron beam used in the production of x-rays in a conventional x-ray source (*11*). An alternative approach is to orient a specimen in a magnetic field and then remove it for study. For dilute solutions this approach is impractical because, once the solution is removed from the field, orientation of the particles decays. X-ray exposure appears to hasten this decay.

Orientation of the specimen can be maintained on removal from a magnetic field if its viscosity is substantially increased while in the field. Stable, highly oriented fibers of filamentous bacteriophages have been produced by partial drying of relatively dilute solutions (30 to 50 mg/ml) (*3, 4, 12*) to

M. J. Glucksman and L. Makowski, Department of Biochemistry and Molecular Biophysics, Columbia University, New York, NY 10032.
R. D. Hay, 12 Holden Wood Road, Concord, MA 01862.

concentrations of 300 to 500 mg/ml. Production of these samples takes days or weeks in a high-field magnet (35 to 100 kG) because the virus concentration must increase slowly for the orientation to be maintained as the specimen dries. The resulting specimens may be appropriate for high-resolution structural studies, but many experiments of interest are better performed in relatively dilute solutions. The milieu of the particles can be precisely and continuously controlled within the same specimen, and changes in structure occurring as a result of the altered environment can be monitored by x-ray diffraction.

Our approach was to place dilute solutions of macromolecular assemblies such as filamentous viruses in a small permanent magnet that produces a field of about 16 kG in a volume of about 1 mm^3. The small size of the magnet assembly allows it to be mounted on a goniometer and used on most x-ray cameras. The 16-kG field is sufficient to orient many macromolecular assemblies, and the small pole separation limits fringe fields so that they have no effect on our x-ray generator or associated equipment.

Figure 1A shows the permanent magnet assembly. The pole faces adjacent to the gap are shaped to improve field homogeneity. The principal circuit magnetization requirements are in the working gap and iron frame and poles; however, there is also unusable flux bypassing the gap that amounts to a significant portion of the total flux from the magnet. The bias magnets serve to modify these circuit magnetization characteristics and allow the principal magnets to operate at a higher permanent field, thus producing a higher field in the gap. Figure 1B is a cross section through the magnet assembly at the pole gap. The bias magnets are split to provide access to the gap through a hole in the assembly normally used to hold the specimen capillary. The soft-steel return frame is made from two L-shaped pieces to allow adjustment of the pole separation. A maximum field of 18 kG is obtained at a pole separation of 0.5 mm.

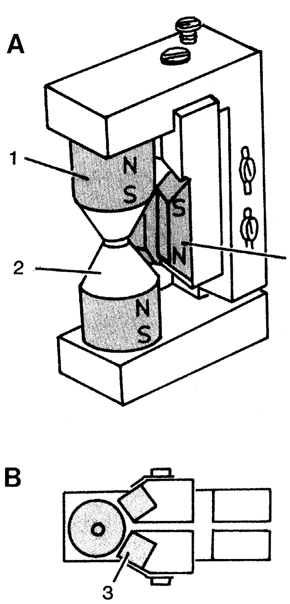

Fig. 1. (A) Side view of the permanent magnet assembly. The overall dimensions of the unit are approximately 50 by 50 by 20 mm. The two principal magnets (1) and the bias magnet (3) are samarium-cobalt permanent magnet material. The pole pieces are soft iron shaped to concentrate the magnetic flux at the pole tips (2). (B) Top view of a cross section through the magnet assembly at the gap. The bias magnets are split to provide access to the gap through a hole in the unit normally used for the specimen capillary. The soft-steel return frame is made from two L-shaped pieces for adjusting the pole separation. Maximum field strength at a pole spacing of 0.5 mm is 18 kG.

Initial x-ray experiments were performed with solutions of filamentous bacteriophages Pf1, M13, and f1. The specimen solution was drawn into a thin-walled siliconized quartz capillary (0.7 mm in diameter) until it occupied a length of 1 to 2 cm in the capillary. The capillary was placed between the poles of the magnet with its axis perpendicular to the magnetic field and going through the access hole. Orientation was monitored by observing the specimen, while in the magnetic field, with a dissecting microscope equipped with polarizers. When fully oriented, the portion of the specimen between the pole pieces exhibited bright birefringence when observed with the magnetic field oriented at 45° to the axes of crossed polarizers (Fig. 2A) and essentially complete extinction when observed with the magnetic field parallel to the axis of one polarizer (Fig. 2B). Material from the same specimen outside the gap did not exhibit this optical behavior, indicating that in the absence of a magnetic field the orientation of the particles was random. Solutions with concentrations of less than 10 mg/ml oriented immediately. Because of strong scattering of x-rays by solvent in the specimens, which were at least 95 percent water by weight, it was necessary to use the most concentrated solutions that oriented in the field. The highest concentration at which a solution oriented varied with the specimen being studied. For the filamentous phages—depending on the virus strain, *p*H, and ionic strength—this concentration was between 30 and 60 mg/ml. Orientation was better for specimens in low ionic strength at *p*H values removed from the isoelectric point of the particle being studied. At the highest orientable concentrations, the solutions often took several hours to orient completely.

Once orientation (as judged by birefringence) was complete, the magnet assembly was mounted on the x-ray cameras, and a 0.5-mm lead aperture was attached to the magnet assembly as close to the specimen as possible on the side toward the x-ray source.

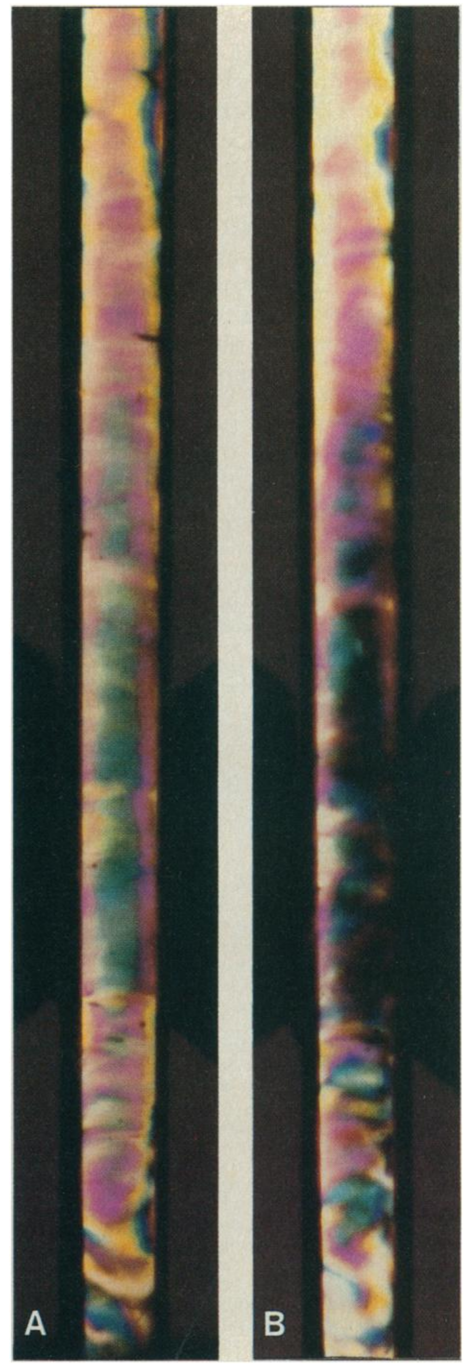

Fig. 2. Photomicrographs of filamentous bacteriophage Pf1 in the permanent magnet between crossed polarizers. The pole pieces of the magnet can be seen on either side of the 0.7-mm-diameter capillary. The bacteriophage exhibits orientation in the region of highest magnetic field between the pole pieces and portions of the capillary immediately adjacent to the pole pieces. (A) Crossed polarizers oriented 45° to the capillary axis. (B) Crossed polarizers oriented parallel and perpendicular to the capillary axis. [Photograph by H. J. Radzyner]

The aperture substantially reduced background due to scattering of x-rays from air and camera components. Diffraction patterns were recorded with a specimen-to-film distance of about 8 cm and exposure times of 2 to 3 days (when a rotating anode x-ray source was used) and 4 to 6 minutes (when the Cornell High-Energy Synchrotron Source was used).

Figure 3 shows three x-ray diffraction patterns from flexible, single-stranded DNA phages about 60 Å in diameter (*13*). The strain Pf1 is nearly 20,000 Å long. Strains M13, f1, and fd are about 9000 Å long, but by subcloning exogenous DNA into their genome, the length of the particle can be increased since it is proportional to the size of the total genome. The diffraction pattern in Fig. 3A is from a specimen of Pf1 (20 mg/ml solution) in the absence of a magnetic field. The diffraction pattern is nearly circularly symmetric. The slight deviation from circular symmetry reflects a weak preference in the phage particles to orient parallel with one another in small domains. Figure 3B shows a Pf1 specimen (18 mg/ml solution) within the magnet assembly. The relatively small amount of arcing of intensity peaks around the center of the pattern demonstrates that the specimen was well oriented in the magnetic field. The half-width of orientation of phage particles in the magnetically oriented solution was about 5°, as judged by measuring arcing of x-ray reflections about the center of the pattern. The separation of intensities along adjacent layer lines was sufficient that accurate intensities could be measured to nearly 7-Å resolution by angular deconvolution of this diffraction pattern (*10*).

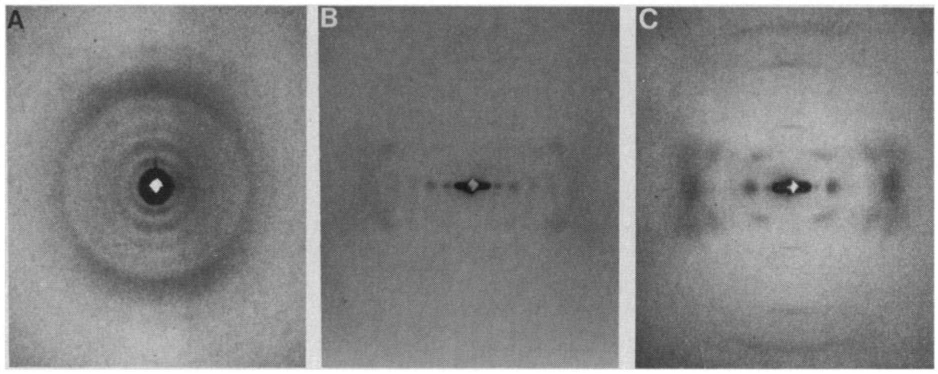

Fig. 3. X-ray diffraction patterns from dilute solutions of filamentous bacteriophages in the presence and absence of a 16-kG magnetic field. (A) A 2 percent solution (20 mg/ml) of filamentous bacteriophage Pf1 in the absence of a magnetic field. The diffraction pattern is nearly circularly symmetric. The slight deviation from circular symmetry is due to a slight preference for the long phage particles to orient parallel to one another in large domains. (B) A magnetically oriented solution of Pf1 (18 mg/ml). Strong equatorial diffraction extending horizontally from the center of the pattern contains information about the radial virion structure. The strongest diffraction is at about 10-Å spacing near the equator and 5-Å spacing along the meridian. [Diffraction pattern taken by L. Specthrie] (C) Magnetically oriented filamentous bacteriophage f1 (40 mg/ml). The layer line spacing is 1/32 $Å^{-1}$, and individual layer lines are well separated to beyond 7-Å spacing. All diffraction patterns are reproduced on the same scale in reciprocal space. The direction of the magnetic field in (B) and (C) is vertical.

The orientation of layer lines perpendicular to the magnetic field indicates that the phage particles orient with their long axes parallel to the field. Figure 3C is a diffraction pattern from M13 (55 mg/ml solution) with a 5.5-kilobase plasmid DNA fragment ligated into its genome to make it about 80 percent longer than native phage. These longer phages were found to orient better than the shorter, native phage particles. The disorientation in the M13 specimen is comparable to that in the specimen of Pf1. Accurate measurement of intensities along all layer lines in these diffraction patterns was possible to nearly 7-Å resolution by angular deconvolution (*10*). Thus, it is possible to obtain a great deal of structural information from diffraction patterns from these oriented solutions.

This method is most promising for the study of the structural changes of macromolecular assemblies in solution. Other types of specimens, such as crystals or partially dried fibers formed by slow drying in a strong magnetic field (>30 kG), may be more useful for high-resolution experiments. In a tightly packed fiber, however, motions of the particles are constrained. For instance, filamentous bacteriophage Pf1 undergoes a structural transition at about 8°C, but this transition does not occur in phage packed into partially dried fibers (*14*). Small changes in the small-angle scattering of Pf1 above and below the transition temperature indicate that the transition can be studied by diffraction from magnetically oriented solutions (*15*).

Comparable results were obtained with neutron diffraction from dilute solutions of filamentous phages by means of a 20-kG magnetic field produced by a large electromagnet. For these experiments, a pole separation of 1.5 to 3.0 cm was necessary to accommodate the much larger specimens required for neutron diffraction. For specimens of filamentous phage fd, the half-width of disorientation observed by neutron diffraction from a specimen 1 cm by 1 cm by 0.25 cm was similar to the half-width of disorientation observed by x-ray diffraction from specimens in 0.7-mm-diameter quartz capillaries as described here. Therefore, the size of the specimen does not appear to affect the degree of magnetic orientation.

The orientation of macromolecular assemblies in a magnetic field is due to their anisotropic magnetic susceptibility. In the filamentous phages, the effect has been attributed to the diamagnetic anisotropy of the peptide bonds in the α helices of the coat protein (*1*). Other planar chemical groups such as nucleotide bases, aromatic rings, and porphyrin rings may contribute to the anisotropic magnetic properties of macromolecular assemblies. Recently it has been shown that small "spherical" plant viruses have a preferred orientation in a magnetic field, apparently due to the organization of RNA within the protein shell (*16*). The torque on an assembly in a magnetic field is opposed by thermal motion, so that the greater the number of chemical groups orienting cooperatively, the higher the degree of orientation. Thus, particles containing a large number of magnetically anisotropic groups are likely to orient better than particles with a small number of groups (*17*). Particles with highly anisotropic shape, such as helical viruses or large flat membrane plaques, may orient better in a magnetic field because the orientations of adjacent particles are not independent of one another. For this reason, better orientation may be found at high concentrations and low ionic strengths. However, the viscosity of concentrated solutions may prevent orientation on an experimentally reasonable time scale. It may be necessary to try many conditions to obtain optimum orientation in a magnetic field. We have demonstrated a simple way of taking advantage of magnetic orientation to greatly increase the amount of structural information obtainable from x-ray diffraction patterns from magnetically oriented solutions. It is possible that a similar approach can be adapted to other biophysical techniques that would benefit from oriented specimens.

REFERENCES AND NOTES

1. Anisotropy in diamagnetic susceptibility is found in organic materials in which bond resonance occurs in a planar group of atoms such as an aromatic group [L. Pauling, *J. Chem. Phys.* 4, 673 (1936)] or a peptide bond [D. L. Worcester, *Proc. Natl. Acad.*

Sci. U.S.A. 75, 5475 (1978); L. Pauling, *ibid.* 76, 2293 (1979)]. Diamagnetic susceptibility will be abnormally large in the direction perpendicular to the planar surface of these groups. When placed in a magnetic field, they will tend to orient with the axis of smallest diamagnetic susceptibility parallel to the external field; that is, the plane of the group will be parallel to the field. This orientation minimizes the energy of the magnetic moment of the group induced by the field and will be the lowest energy orientation of the group. Aromatic groups and peptide bonds will tend to orient parallel to an external field. Because of the orientation of peptide bonds within them, α helices and β sheets will tend to orient parallel to a magnetic field.
2. J. Torbet and G. Maret, *J. Mol. Biol.* **134**, 843 (1979).
3. D. W. Banner, C. Nave, D. A. Marvin, *Nature (London)* **289**, 814 (1981).
4. C. Nave *et al.*, *J. Mol. Biol.* **149**, 675 (1981).
5. M. Chabre, *Biochim. Biophys. Acta* **382**, 322 (1975).
6. J. M. Freyssinet, J. Torbet, G. Hudry-Clergeon, G. Maret, *Proc. Natl. Acad. Sci. U.S.A.* **80**, 1616 (1983); J. Torbet, J. M. Freyssinet, G. Hudry-Clergeon, *Nature (London)* **289**, 91 (1981).
7. D.-Ch. Neugebauer, A. E. Blaurock, D. O. Worcester, *FEBS Lett.* **78**, 31 (1977).
8. G. Maret, M. V. Schickfus, A. Mayer, K. Dransfeld, *Phys. Rev. Lett.* **35**, 397 (1975).
9. P. Costa Ribeiro, M. A. Davidovich, E. Wajnberg, G. Bemsk, M. Kishinevsky, *Biophys. J.* **36**, 443 (1981).
10. L. Makowski, *J. Appl. Crystallogr.* **11**, 273 (1978).
11. W. C. Philips, *ibid.* **13**, 338 (1980).
12. L. Makowski, in *Biological Macromolecules and Assemblies*, F. A. Jurnak and A. Mcpherson, Eds. (Wiley, New York, 1984), vol. 1, pp. 203–254.
13. D. A. Marvin, W. J. Pigram, R. L. Wiseman, E. J. Wachtel, F. J. Marvin, *J. Mol. Biol.* **88**, 581 (1974).
14. E. J. Wachtel, F. J. Marvin, D. A. Marvin, *ibid.* **107**, 379 (1976); C. Nave *et al.*, *Nature (London)* **281**, 232 (1979).
15. L. Specthrie, J. Greenberg, M. J. Glucksman, L. Makowski, *Ann. N.Y. Acad. Sci.*, in press.
16. J. Torbet, *EMBO J.* **2**, 63 (1983).
17. Cloning exogenous DNA into a filamentous phage genome yields a virus particle with a length increase proportional to the size of the insert. Our observations of M13 and f1 phage particles with lengths up to 80 percent greater than native phage have indicated a negative correlation between the length of these phages and the time needed for them to orient in a given magnetic field under the conditions used.
18. We thank P. Model and M. Russel for providing us with a strain of f1, B. Schoenborn and A. M. Saxena for help and use of facilities at the Brookhaven Neutron Source, and K. Moffat for aid in synchrotron experiments. Supported by NIH grants GM29829 and GM34343.

3 September 1985; accepted 16 December 1985

1981N1: A Neptune Arc?

W. B. HUBBARD

An object in the vicinity of Neptune detected in 1981 by simultaneous stellar occultation measurements at observatories near Tucson, Arizona, was interpreted as a new Neptune satellite. A reinterpretation suggests that it may have instead been a Neptune arc similar to one observed in 1984. The 1981 object, however, did not occult the star during simultaneous observations at Flagstaff, Arizona. This result constrains possible arc geometries.

IN 1981, SIMULTANEOUS PHOTOMETRY of a stellar appulse to Neptune observed from two telescopes in Arizona 6 km apart revealed a previously undiscovered occulting object at a distance of about 3 Neptune radii (3 R_N) from the planet's center (*1*). The object, which was given the temporary designation 1981N1, was found to be essentially opaque, with sharp, well-defined edges (Fig. 1). The contribution of the star to the blue signal (Fig. 1, b and d) was negligible; thus no occultation is visible here. The events in Fig. 1, a and c, correspond to a drop of approximately 100 percent in the stellar intensity, although, since the star was only 3 to 4 percent of the total red signal, this is difficult to determine with great precision. The original interpretation of these events was that they were caused by a previously undiscovered third Neptune satellite with a diameter in the range of 100 to 1000 km.

No further confirmed detections of material near Neptune were reported until 22 July 1984, when observers at three telescopes in Chile carried out simultaneous observations of the appulse of a bright star (SAO 186001) to Neptune. All three stations recorded a nearly simultaneous event near 5 hours, 40 minutes universal time (U.T.) (*2*). The 1984 event did not have sharp edges, nor was the star fully occulted at any time, and therefore the occulter could not have been a single solid satellite with any plausible shape. The duration of the event and its nearly identical nature at stations separated by 100 km implied that the occulting object was an arc of a partially (about 68 percent) transparent ring centered on Neptune with a radial width of about 15 km (*3*). The 1984 object was azimuthally coherent over at least 100 km, but, like the 1981 event, it was clearly not a large-scale ring since no corresponding occultation event occurred at the expected second crossing point. The 1984 arc was at a radial distance of about 67,000 ± 4,000 km (2.7 R_N) from the center of the planet, assuming that it was in Neptune's equatorial plane. The radial distance was computed from photographic astrometric data on the relative positions of Neptune and the star, and the error bar reflects the uncertainty in applying these data to computation of the occultation track (*3*).

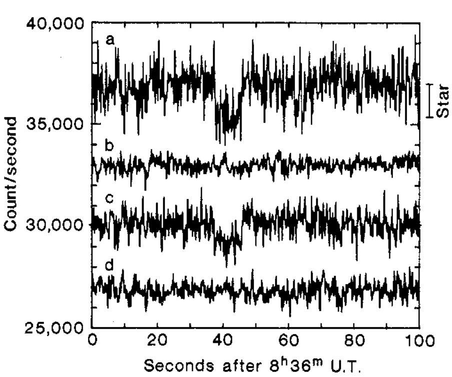

Fig. 1. Detections of 1981N1 from the 1.54-m Catalina Station telescope and from the 1-m Mt. Lemmon telescope 6 km distant on 24 May 1981, at a time resolution of 0.2 second (*1*). The traces show the combined signal of Neptune plus the uncataloged star as a function of time. Here (a) and (c) are, respectively, the red-channel signals at the 1.54-m and 1-m telescopes, multiplied by factors of 4.0 and 1.95; (b) and (d) are the blue-channel signals, multiplied by factors of 0.143 and 0.310.

1981N1 was originally interpreted to be a single satellite. However, the probability of the detection of a single small satellite by random occultation is clearly very small, whereas an extensive system of incomplete arcs would be likely to have a much higher probability of detection (perhaps of order 10 percent, judging from statistics on Neptune occultations observed to date). This circumstance suggests that the 1981 events may not have been caused by an isolated satellite but instead represented an early detection of a Neptunian arc.

Could the 1981 object have been a Neptune arc, much wider and more opaque than the 1984 arc? One way to test this hypothesis is to exploit the well-defined immersion and emersion times of the 1981 occultation events to calculate the location of the occultation points in the sky reference plane centered on Neptune, assuming that the occulting object has the same orbital velocity vector as Neptune. If the occulter was an arc, then the lines defined by the two immersion points and the two emersion points respectively should be parallel and should have a position angle consistent with that of an equatorial concentric arc. With a station

Lunar and Planetary Laboratory, University of Arizona, Tucson 85721.